EARTH OBSERVATION AND GEOMATICS ENGINEERING
website: https://eoge.ut.ac.ir

On the evaluation of second order phase statistics in SAR interferogram stacks

Sami Samiei-Esfahany*, Ramon Hanssen

Department of Geoscience and Remote Sensing, Delft University of Technology, Delft, the Netherlands

Article history:
Received: 20 November 2016, Received in revised form: 1 April 2017, Accepted: 10 April 2017

ABSTRACT

During the last decades, time-series interferometric synthetic aperture radar (InSAR) has been emerged as a powerful technique to measure various surface deformation phenomena of the earth. The multivariate statistics of interferometric phase stacks plays an important role in the performance of different InSAR methodologies and also in the final quality description of InSAR derived products. The multivariate phase statistics are ideally described by a joint probability distribution function (PDF) of interferometric phases, whose closed-form evaluation in a generic form is very complicated and is not found in the literature. Focusing on the first two statistical moments, the stack phase statistics can be effectively described by a full (co)variance matrix. Although a closed-form expression of interferometric phase variances has been derived in literature for single-looked pixels, there is no such an expression for neither the variances of the multilooked pixels nor the covariances among interferometric phases. This paper presents two different approaches for evaluation of the full covariance matrix: one based on the numerical Monte-Carlo integration and the other based on an analytical approximation using nonlinear error propagation. We first, clarify on the noise components that are the subject of statistical models of this paper. Then, the complex statistics in SAR stacks and the phase statistics in a single interferogram are reviewed, followed by the phase statistics in InSAR stacks in terms of second statistical moments. The Monte-Carlo approach and the derivation of an analytical closed-form evaluation of InSAR second-order phase statistics are then introduced in details. Finally, the two proposed methods are validated against each other.

KEYWORDS

InSAR
Covariance matrix
Radar interferometry
Phase statistics

1. Introduction

Since the late 1990s, different methodologies have been developed for processing multi-baseline Interferometric Synthetic Aperture Radar (InSAR) data stacks. Except for some recently developed algorithms (Ferretti et al., 2011; Monti-Guarnieri & Tebaldini, 2008) which are based on direct processing of SAR data instead of processing interferograms, most other algorithms use interferometric phases as primary inputs. Therefore, the phase statistics of interferograms (i.e., noise characteristics of interferometric phases) can play an important role in performance of different InSAR methodologies. For example, these statistics can be used for maximum likelihood estimation of different parameters of interest such as deformation, deformation rate, and topography, and can also be used for uncertainty (precision and reliability) description of these products. The phase statistics are ideally described by a probability distribution function (PDF) of interferometric phases. This PDF is a function of absolute interferometric coherence, which is a measure of the accuracy of the interferometric phase. In the case of a single interferogram, this PDF was derived in the closed form for both single and multi-looked cases in Bamler & Hartl (1998), Tough (1995), Just & Bamler (1994), Lee et al. (1994), Rodriguez & Martin (1992), Sarabandi (1992). However, in case of multi-baseline interferograms, we are dealing with a complicated multi-dimensional joint PDF of interferometric phases. Such a joint PDF is difficult to derive and exploit, not only because of its high dimensionality but also because of the highly nonlinear relationship between the interferometric phases and the acquired complex SAR data. For simplicity, this PDF is usually computed based on the harsh assumption of mutual independency between interferograms, for example in Eineder & Adam (2005) and Cuenca et al. (2011). In this case, the joint PDF of multiple interferograms would be the product of PDFs of the single interferograms. However, this

* Corresponding author
E-mail addresses: s.samieiesfahany@tudelft.nl (S. SamieiEsfahany); r.f.hanssen@tudelft.nl (R.F. Hanssen)
DOI: 10.22059/eoge.2017.63865.1016

independency assumption is not always met, especially because of the correlation of noise components between interferograms. Also two interferograms with a common SAR acquisition can never be independent, since they both depend on the common image signal. Some efforts has been found in literature for evaluation of the joint PDF of multi-baseline interferograms. Lucido et al. (2010) presented the closed-form evaluation of the second-order joint PDF for two interferograms only, obtained by three correlated SAR images and for the single-looked case. No such study has been found for more general cases, i.e., for any two interferograms and for different multi-looking factors. Another convenient way to describe the phase statistics, especially for near-Gaussian data is to focus just on the first two statistical moments and use the covariance matrix of interferometric phases instead of the full joint PDF. In this way, instead of a complicated N-dimensional joint PDF (assuming N as number of SAR images), we are dealing with an $N\times N$ covariance matrix which is more convenient to exploit in practice. Diagonal elements of such a matrix are variances of interferometric phases and off-diagonal elements are the covariances which describe the dependency among interferometric phases. The closed-form expression of interferometric phase variances were derived in Bamler & Hartl (1998) and Tough (1995) for the single-looked case. For a multi-looked case, variances can be derived numerically from the PDF. However, for evaluating the covariances, we need again the joint PDF of interferometric phases. Although, as mentioned before, there is a closed-form evaluation of this joint PDF for the simple case (Lucido et al., 2010), there is need for the evaluation of such a PDF for more general cases.

In this paper, we present two approaches for this purpose: one based on the numerical Monte-Carlo integration and the other based on an analytical approximation using nonlinear error propagation. The paper is organized as follows. We first, in Section 2 clarify on the noise components that are the subject of statistical models of this paper. Then, we revisit the complex statistics in SAR stacks (Section 3). In addition, the phase statistics in a single interferogram are reviewed (Section 4), followed by the phase statistics in InSAR stacks in terms of second statistical moments or in the form of a covariance matrix (Section 5). A Monte-Carlo methodology to compute a full covariance matrix for interferometric phase stacks is introduced (Section 5.4), followed by the derivation of an analytical closed-form evaluation of InSAR second-order phase statistics (Section 5.5). The conclusions and summary are given in (Section 6).

2. Noise components in SAR/InSAR stacks

In general, the stochastic model of observations describes the uncertainty in the measurements by means of some statistical tools. Our main focus in this paper is on the stochastic aspects of noise/error components in SAR and InSAR stacks with special attention to DS-pixels. The term "noise", however, may be interpreted loosely as its definition is application-dependent: *one man's signal is the other man's noise*. From the four main components of SAR/InSAR phase observations (i.e. the range-dependent component, atmospheric signal, the scattering effect, and noise), the range dependent phase is defined as a signal that includes information about the deformation and topography of the imaged area, and it is usually modeled functionally and is considered deterministic (or sometimes it is modeled as the summation of a deterministic model and stochastic deviations from the model), e.g., in Hanssen (2001), Ferretti et al. (2001), and Kampes & Hanssen (2014). The other components are usually modeled in a statistical sense by means of a probability distribution function (PDF) or its first two statistical moments. Based on the different spatio-temporal behavior of SAR/InSAR stochastic components, we analyze and model them independently. The scattering effect and the system noise mainly affect every single resolution-cell independently, resulting in an insignificant spatial correlation among nonadjacent pixels. Therefore, the stochastic model for these components can be presented in the single-point level. In contrary, the atmospheric components (and the unmolded deformation) have strong spatial correlation (Hanssen, 2001), and therefore, their stochastic model can be defined for multiple-points. As suggested by Hanssen (2001), focusing on 2nd statistical moments, the full covariance matrix of SAR/InSAR measurements Q can be approximated as summation of a covariance matrix Q_n influenced by single-point statistics and an atmospheric covariance matrix Q_{atmo} affected by multiple-point statistics as:

$$Q \doteq Q_{\mathrm{n}} + Q_{\mathrm{atmo}} \tag{1}$$

The key focus in this paper is on the evaluation/description of single-point statistics for distributed scatterers (DS) pixels. The reason is mainly that the multiple-point stochasticity mainly describes the variability in atmospheric effects and is described comprehensively in literature, see for example Hanssen (2001).

3. Single-point complex statistics for DS in SAR stacks

3.1 Physical origin of noise

The reflected signal received from a DS resolution cell is equal to the coherent summation of the reflections from multitude of elementary scatterers within the cell. In other words, the complex value (phasor) P of a pixel (with amplitude A and phase(ψ) can be written as the complex summation of the phasors of all the elementary scatterers within the associated resolution cell:

$$\mathrm{P}=\mathrm{A}\exp(j\psi)=\sum_i S_i=\sum_i a_{\mathrm{i}}\exp(\varsigma_i)=\sum_i \Re(S_i)+j\sum_i \Im(S_i) \tag{2}$$

where S_i, a_{i}, and ς_i are the phasor, amplitude, and phase of the ith elementary scatterer within the cell. The elementary scattering phase ς_i is a function of the relative position and dielectric characteristics of each elementary scatterer. Although the complex phasor P and its phase and amplitude are intrinsically deterministic quantities, i.e. they are invariant if the measurements are repeated under the same condition, they are unpredictable and hence they cannot be described mathematically in a deterministic manner, and so they are modeled stochastically. Assuming the location and distribution of elementary scatterers within a resolution cell to be random, the summation of S_i values should result in a phasor P with a Wiener (or random walk) process (Sarabandi, 1992; Davenport, 1970). For a large number of

elementary scatterers, based on the central limit theorem[1], the phasor P is a complex random variable with a circular Gaussian distribution (Sarabandi, 1992; Madsen, 1986).

3.2 Circular Gaussian distribution

Goodman (1976) Showed that, under certain assumptions, the complex SLC phasor P has a zero-mean[2] circular Gaussian distribution. These assumptions are (Bamler & Hartl, 1998; Madsen, 1986; Goodman, 1976):

1. the responses of all the elementary scatterers within the resolution cell are independent,
2. for each elementary scatterer, the amplitude A_i and phase ς_i are independent,
3. the phases ς_i are uniformly distributed between -π and π, and
4. All the elementary scatterers produce comparable amplitudes A_i — there is no dominant scatterer within a resolution cell.

These assumptions generally hold for areas with a surface roughness comparable to the radar wavelength, and for DS-pixels over homogeneous natural landscapes such as agricultural fields, forests, and deserts. Considering a single DS-pixel in a stack of N SAR images, the set of phasors in all the images can be seen as a multivariate complex random variable $\underline{y}=[\underline{P}_1\ \underline{P}_2\cdots\underline{P}_N]^T$. The zero-mean circular complex Gaussian PDF of $\underline{y}$ is written as (Lee et al., 1994; Goodman, 1976; Hannan & Thomson, 1971).

$$f_{\underline{y}}(y)=\frac{1}{\pi^N|Q_y|}\exp(-y^*Q_y^{-1}y) \tag{3}$$

where $Q_y=\mathrm{D}\{\underline{y}\}=\mathrm{E}\{\underline{y}\,\underline{y}^*\}$ is an $N\times N$ complex covariance matrix defined by Eq. (4).

$$Q_y=\begin{bmatrix} \mathrm{E}\{|\underline{P}_1|^2\} & \gamma_{12}\sqrt{\mathrm{E}\{|\underline{P}_1|^2\}\mathrm{E}\{|\underline{P}_2|^2\}} & \cdots & \gamma_{1N}\sqrt{\mathrm{E}\{|\underline{P}_1|^2\}\mathrm{E}\{|\underline{P}_N|^2\}} \\ \gamma_{12}^*\sqrt{\mathrm{E}\{|\underline{P}_1|^2\}\mathrm{E}\{|\underline{P}_2|^2\}} & \mathrm{E}\{|\underline{P}_2|^2\} & \cdots & \gamma_{2N}\sqrt{\mathrm{E}\{|\underline{P}_2|^2\}\mathrm{E}\{|\underline{P}_N|^2\}} \\ \vdots & \vdots & \ddots & \vdots \\ \gamma_{1N}^*\sqrt{\mathrm{E}\{|\underline{P}_1|^2\}\mathrm{E}\{|\underline{P}_N|^2\}} & \gamma_{2N}^*\sqrt{\mathrm{E}\{|\underline{P}_2|^2\}\mathrm{E}\{|\underline{P}_N|^2\}} & \cdots & \mathrm{E}\{|\underline{P}_N|^2\} \end{bmatrix} \tag{4}$$

in this formulation, the γ values are the complex correlation coefficients (called coherence values) between pair of images. The coherence value between P_i and P_j is defined as (Born et al., 1959; Foster & Guinzy, 1967 ; Papoulis, 1991).

$$\gamma_{ij}=\frac{\mathrm{E}\{\underline{P}_i\underline{P}_j^*\}}{\sqrt{\mathrm{E}\{|\underline{P}_i|^2\}\mathrm{E}\{|\underline{P}_j|^2\}}}=|\gamma_{ij}|\exp(j\phi_{0_{ij}}) \tag{5}$$

where the phase of the complex coherence, $\phi_{0_{ij}}\in[-\pi,\pi)$, is the phase of the expectation of the complex interferometric product $\underline{P}_i\underline{P}_j^*$. The absolute coherence $|\gamma_{ij}|\in[0,1]$ is a measure of the correlation between the noise components of P_i and P_j. When the coherence is high, the noise components in P_i and P_j have a higher similarity, and so a large portion of the noise components will be canceled out in the interferometric phase. Consequently, the absolute coherence is also a normalized measure of the dispersion of the interferometric phase noise. The complex correlation matrix of the vector $\underline{y}$ is called the coherence matrix and is defined as:

$$\Gamma_y=\begin{bmatrix} 1 & \gamma_{12} & \cdots & \gamma_{1N} \\ \gamma_{12}^* & 1 & \cdots & \gamma_{2N} \\ \vdots & \vdots & \ddots & \vdots \\ \gamma_{1N}^* & \gamma_{2N}^* & \cdots & 1 \end{bmatrix} \tag{6}$$

note that the coherence matrix Γ_y is a Hermitian matrix[3]. Using the definition of the coherence matrix Eq. (6), the covariance matrix Q_y (see Eq. (4)) can be reformulated as:

$$Q_y=\Gamma_y\circ\underbrace{\begin{bmatrix} \mathrm{E}\{|\underline{P}_1|^2\} & \sqrt{\mathrm{E}\{|\underline{P}_1|^2\}\mathrm{E}\{|\underline{P}_2|^2\}} & \cdots & \sqrt{\mathrm{E}\{|\underline{P}_1|^2\}\mathrm{E}\{|\underline{P}_N|^2\}} \\ \sqrt{\mathrm{E}\{|\underline{P}_1|^2\}\mathrm{E}\{|\underline{P}_2|^2\}} & \mathrm{E}\{|\underline{P}_2|^2\} & \cdots & \sqrt{\mathrm{E}\{|\underline{P}_2|^2\}\mathrm{E}\{|\underline{P}_N|^2\}} \\ \vdots & \vdots & \ddots & \vdots \\ \sqrt{\mathrm{E}\{|\underline{P}_1|^2\}\mathrm{E}\{|\underline{P}_N|^2\}} & \sqrt{\mathrm{E}\{|\underline{P}_2|^2\}\mathrm{E}\{|\underline{P}_N|^2\}} & \cdots & \mathrm{E}\{|\underline{P}_N|^2\} \end{bmatrix}}_{\bar{I}} \tag{7}$$

where ∘ represents the Hadamard (i.e., entry-wise) product, and the matrix $\bar{I}$ is the expectation power matrix whose elements are defined by

$$\bar{I}_{[i,j]}=\zeta_{ij}=\sqrt{\zeta_{ii}\zeta_{jj}}=\sqrt{\mathrm{E}\{|\underline{P}_i|^2\}\mathrm{E}\{|\underline{P}_j|^2\}} \tag{8}$$

4. Single-point phase statistics for single interferogram

In the previous section the single-point phase statistics of distributed scatterers in SAR stacks were discussed. In order to evaluate the single-point interferometric phase statistics, the SAR statistics should be propagated through the interferogram generation process which includes complex conjugate multiplication of pairs of SAR images. Here, we first look at the phase statistics for a single interferogram, followed in Section 5, by the extension of the stochastic model to the multi-interferogram case, i.e., for a vector of single-point interferometric phases in InSAR stacks. Assuming two SLC pixels P_1 and P_2 with zero-mean complex circular Gaussian distribution (see Eqs. (3) and (4)), with complex coherence γ (see Eq. (5)), the joint PDF of the amplitude and the phase of the multilooked interferogram constructed from the two SLC images is given by (Tough, 1995; Lee et al., 1994; Goodman, 1963; Barber, 1993):

[1] Central limit theorem: Let $\underline{x}_1,\cdots\underline{x}_n$ be independent random variables/vectors and let $\underline{z}=\sum_{i=1}^{n}\underline{x}_i$. Then under general conditions, the distribution of $\underline{z}$ approaches the (multivariate) normal distribution as n increases ($n\to\infty$).

[2] Here zero-mean refers to representation in real and imaginary components of the phasor.

[3] A Hermitian matrix is a complex square matrix that is equal to its own conjugate transpose. Hermitian matrices are the complex counterparts of symmetric matrices for real numbers. Note that the real part (and the absolute) of a Hermitian matrix is a symmetric matrix, but its imaginary part (and its phase) is a skew-symmetric matrix: its transpose is equal to its negative.

$$f_{\underline{A},\underline{\phi}}(A,\phi)=\frac{2L(LA)^L}{\pi\zeta^{L+1}(1-|\gamma|^2)\Gamma(L)}\exp\left(\frac{2|\gamma|LA\cos(\phi-\phi_0)}{\zeta(1-|\gamma|^2)}\right)K_{L-1}\left(\frac{2LA}{\zeta(1-|\gamma|^2)}\right) \quad (9)$$

where L is the number of looks, $K_{L-1}(.)$ the modified Bessel function of the third kind (Gradshteyn et al., 1994), $\Gamma(.)$ the Gamma function, and $\zeta=\sqrt{\mathrm{E}\{|P_1|^2\}\mathrm{E}\{|P_2|^2\}}$. By integrating over amplitudes A, the marginal PDF of the interferometric phase ϕ is computed as Bamler & Hartl (1998).

$$f(\phi)=\frac{(1-|\gamma|^2)^L}{2\pi}\left\{\frac{\Gamma(2L-1)}{(\Gamma(L))^2\,2^{2(L-1)}}\times\left\{\frac{(2L-1)\beta}{(1-\beta^2)^{L+0.5}}\left(\frac{\pi}{2}+\arcsin(\beta)\right)+\frac{1}{(1-\beta^2)^L}\right\}+\frac{1}{2(L-1)}\sum_{r=0}^{L-2}\frac{\Gamma(L-0.5)}{\Gamma(L-0.5-r)}\frac{\Gamma(L-1-r)}{\Gamma(L-1)}\frac{1+(2r+1)\beta^2}{(1-\beta^2)^{r+2}}\right\} \quad (10)$$

with $\beta=|\gamma|\cos(\phi-\phi_0)$, where ϕ_0 is the expected interferometric phase. An equivalent formulation of $f_{\underline{\phi}}(\phi)$ has been presented in different publications (Lee et al., 1994; Barber, 1993, Joughin & Winebrenner, 1994; Lucido et al., 2010).

$$f_{\underline{\phi}}(\phi)=\frac{\Gamma(L+0.5)(1-|\gamma|^2)^L\beta}{2\sqrt{\pi}\Gamma(L)(1-\beta^2)^{L+0.5}}+\frac{(1-|\gamma|^2)^L}{2\pi}\,{}_2F_1(L,1;0.5;|\gamma|^2\beta^2)\quad -\pi\le\phi<\pi \quad (11)$$

where ${}_2F_1(.)$ is the classical standard hypergeometric function (Kampes & Hanssen, 2004; Oberhettinger, 1970). For single-look pixels (i.e., L=1), the interferometric phase PDF reduces to (Tough et al, 1995; Just & Bamler, 1994; Lee et al., 1994):

$$f_{\underline{\phi}}(\phi|L=1)=\frac{(1-|\gamma|^2)((1-\beta^2)^{0.5}+\beta(\pi-\cos^{-1}(\beta)))}{2\pi(1-\beta^2)^{1.5}}\quad -\pi\le\phi<\pi \quad (12)$$

Figures 1A, B, and C show examples of $f_{\underline{\phi}}(\phi)$ for coherence values 0.2, 0.5, and 0.8, evaluated for different number of looks L=1, 5, 10, 20, and 50. We can see that the higher L is, the more peaked the PDF is. For the extreme case of $|\gamma|=0$, $f_{\underline{\phi}}(\phi)$ reduces to

$$f_{\underline{\phi}}(\phi|\gamma|=0)=\frac{1}{2\pi}\quad \text{for}\ -\pi\le\phi<\pi \quad (13)$$

which is equivalent to the PDF of uniformly distributed phases between -π and π. For another extreme scenario of $|\gamma|=1$ (i.e., zero decorrelation or zero noise), the interferometric phase PDF reduces to the Dirac delta function:

$$f_{\underline{\varphi}}(\phi|\ |\gamma|=1)=\begin{cases}\infty & \phi=\phi_0\\ 0 & \phi\neq\phi_0\end{cases} \quad (14)$$

4.1 First and second statistical moments of interferometric phase

With the PDFs of Eqs. (10) or (11), the mean and the variance of the interferometric phases can be computed by evaluating the first two statistical moments of $f_{\underline{\phi}}(\phi)$ as:

$$\mathrm{E}\{\underline{\phi}\}=\mu_{\underline{\phi}}=\int_{-\pi}^{\pi}\phi f_{\underline{\phi}}(\phi)d\phi \quad (15)$$

$$\mathrm{D}\{\underline{\phi}\}=\sigma^2_{\underline{\phi}}=\int_{-\pi}^{\pi}(\phi-\mathrm{E}\{\underline{\phi}\})^2 f_{\underline{\phi}}(\phi)d\phi \quad (16)$$

For the single-look case (i.e.,L=1), Tough et al. (1995) evaluated the integrals of Eqs. (15) and (16) in a closed from as:

$$\mu_{\underline{\phi},L=1}=\frac{|\gamma|\sin(\phi_0)}{\sqrt{1-|\gamma|^2\cos^2(\phi_0)}}\arcsin(|\gamma|\cos(\phi_0)) \quad (17)$$

$$\sigma^2_{(\underline{\phi},L=1)}=\frac{\pi^2}{3}-\pi\arcsin(|\gamma|\cos(\phi_0))+(\arcsin(|\gamma|\cos(\phi_0)))^2-\mathrm{Li}_2(|\gamma|^2) \quad (18)$$

where $\mathrm{Li}_2(.)$ is the Euler's dilogarithm[4]. Note that both aforementioned evaluations of the mean and variance are not only related to $|\gamma|$, but they are also a function of ϕ_0. This fact challenges the interpretation of mean and variance as a metric for the central tendency and spread of the interferometric phase. Ideally we are interested in a measure of central tendency which can characterize ϕ_0, and a measure of dispersion which characterizes the spread of the phase around ϕ_0. However in above equations, for example if ϕ_0 (and consequently the mode of the PDF) deviates from zero, the bounded PDF between -π and π becomes non-symmetric around the mode, and consequently the mean of Eq. (16) is not representative of the central tendency, while the mode is a better measure. In the same manner, the variance is not representative of phase dispersion around ϕ_0, but it is a measure of non-symmetric dispersion around the mean (See Qugan et al. (1994) for more discussion). In fact we are interested in a measure of dispersion which is invariant with respect to ϕ_0 and which depends only on the coherence as a measure of noise. So the central tendency and the measure of phase dispersion ideally should be defined relative to the mode and account for the 2π symmetry of the PDF (Tough, 1995). In order to solve this problem, considering the fact that the phase PDF is periodic with a 2π cycle, it is suggested to evaluate the integration of Eqs. (15) and (16) in the interval $(\phi_0-\pi,\phi_0+\pi)$ instead of (-π,π), resulting in the following definition of phase mean and variance (Just & Bamler, 1994):

[4] Euler's dilogarithm is defined as: $\mathrm{Li}_2(x)=\sum_{i=1}^{\infty}\frac{x^k}{k^2}$

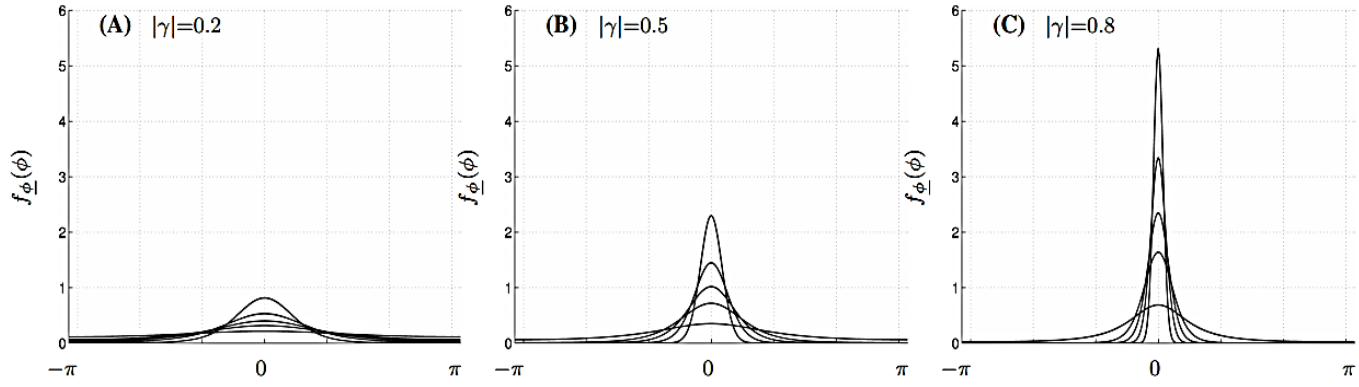

Figure 1. Probability density function of interferometric phase for coherence levels (A) $|\gamma|$=0.2, (B) $|\gamma|$=0.5, and (C) $|\gamma|$=0.8 evaluated for different number of looks L=1, 5, 10, 20, and 50 (the higher the L, the more peaked PDF). It is evident that multilooking improves the precision of the interferometric phase. All the PDFs were computed based on Eq. (11) assuming ϕ_0=0. After Hanssen (2001)

$$E\{\underline{\phi}\}=\mu_{\underline{\phi}}=\int_{\phi_0-\pi}^{\phi_0+\pi}\phi f_{\underline{\phi}}(\phi)d\phi=\phi_0 \quad (19)$$

$$D\{\underline{\phi}\}=\sigma^2_{\underline{\phi}}=\int_{\phi_0-\pi}^{\phi_0+\pi}(\phi-\phi_0)^2 f_{\underline{\phi}}(\phi)d\phi=\int_{-\pi}^{\pi}(\phi)^2 f_{\underline{\phi}}(\phi+\phi_0)d\phi \quad (20)$$

It should be pointed out that changing the integration interval to $(\phi_0-\pi,\phi_0+\pi)$, is equivalent to evaluating the integral in the interval $(-\pi,\pi)$ under the assumption of ϕ_0=0. With this new definition of the mean (i.e. Eq. (19)), $\mu_{\underline{\phi}}$ directly characterizes ϕ_0 and it is independent of the coherence values. Equivalently, the variance of Eq. (20) is now dependent on $f_{\underline{\phi}}(\phi+\phi_0)$ which is invariant with respect to ϕ_0, and so the evaluated variance is exclusively a function of coherence. In general there is no closed-form evaluation of Eq. (20) (Except for single-look cases), and therefore the integral should be evaluated numerically. For single-look cases, the closed-form evaluation of Eq. (20) results in Monti-Guarnieri & Tebaldini (2008):

$$\sigma^2_{\underline{\phi},L=1}=\frac{\pi^2}{3}-\pi\arcsin(|\gamma|)+(\arcsin(|\gamma|))^2-\mathrm{Li}_2(|\gamma|^2) \quad (21)$$

which is equivalent to Eq. (18) if ϕ_0=0. In Figure 2 the standard deviation of the interferometric phase (i.e., $\sqrt{\sigma^2_{\underline{\phi}}}$) is evaluated as a function of coherence $|\gamma|$ and for different number of Looks L=1,10,20, and 50. It is evident that a higher multilooking factor reduces the phase standard deviation, assuming ergodicity. Note that in the highest dispersion case (i.e., $|\gamma|$=0), the standard deviation reaches an upper bound which which is the standard deviation of uniformly distributed phase between -π .

5. Single-point phase statistics for interferogram stack

In the previous section, we discussed the statistical properties of interferometric phases for single pixels in single interferograms. Thus, the interferometric phase is a univariate random variable, with a one-dimensional PDF whose dispersion is given by the phase variance. However, in order to evaluate phase statistics for one pixel in a stack of interferograms, we are dealing with a multivariate vector of interferometric phases, with a multi-dimensional PDF (or a joint PDF of all the interferometric phases for one pixel) and the dispersion in the form of a full covariance matrix. If the decorrelation noise components in different interferograms are assumed independent, the joint PDF can be evaluated simply by multiplication of the univariate phase PDFs given by Eqs. (10) or (11), and the phase dispersion can be described by a diagonal covariance matrix whose diagonal elements are equal to univariate variance factors evaluated by Eq. (18). However the assumption of independency may not hold due to different reasons. In this section, we first discuss the reasons of dependency/correlation between the noise components, followed by reviewing different conceptsfor the analytical and numerical evaluation of multivariate interferometric phase PDFs and their dispersion.

5.1 Causes of correlation between interferograms

Assume two interferograms I_{12} and I_{34} constructed from a set of four SLC images P_1, P_2, P_3, and P_4. In order to evaluate the correlation between the phases of the two interferograms, the noise statistics of the complex multivariate vector $y=[P_1,P_2,P_3,P_4]^T$, which can be described by a circular complex Gaussian distribution (see Eqs. (3) and (5)), should be propagated to the 2×2 covariance matrix of the vector $[\phi_{12},\phi_{34}]^T$. As the SLC values in the vector y are likely to be correlated (as described by coherence values in the 4×4 coherence matrix Γ_y), there is no reason in principle to assume that the two interferometric phases are independent. In fact, the interferometric phases can be correlated or uncorrelated as expressed by different sets of coherence values in Γ_y. In order to get more insight on the physical origin of the correlation between noise components, we discuss three main sources of this dependency in the following[5].

[5] Note that in this paper, we are discussing the statistics of noise terms due to different decorrelation mechanisms (i.e., single-point statistics, see Section 2 for more information on discrimination between different noise components). Therefore, when we talk about correlation or dependency, we mean correlation or statistical dependency between different noise terms for one pixel in two interferograms. This should not be mistakenly interpret as the correlation between other signal/noise components such as atmospheric or deformation phase.

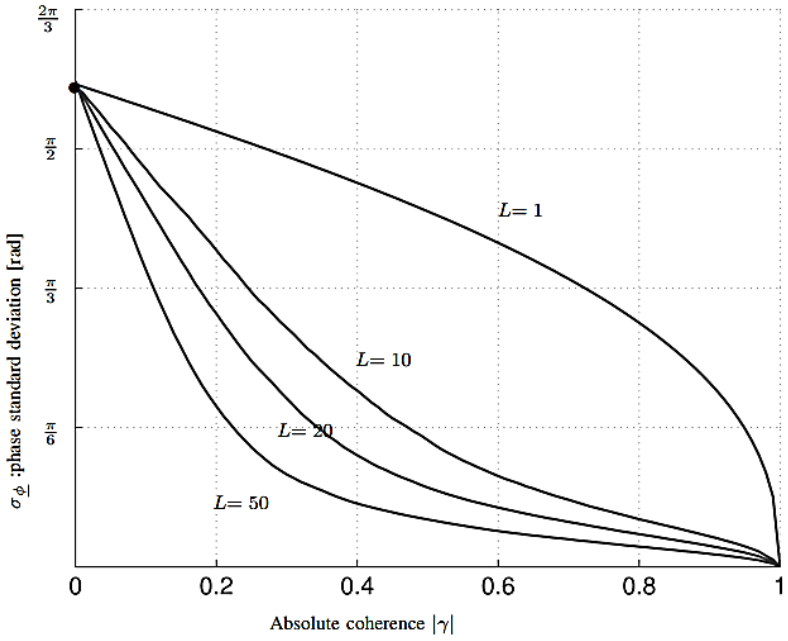

Figure 2. Evaluation of standard deviation of the interferometric phase (σ_ϕ) as a function of coherence $|\gamma|$, for four different number of looks L=1,10,20, and 50. The standard deviations are computed by numerical evaluation of Eq. (20). The upper-bound of standard deviation (visualized by the black dot •) is equivalent to $2\pi/\sqrt{12}$ (or $\approx 104^o$), which is the standard deviation of uniformly distributed phase between $-\pi$ and π. After Tough (1995).

5.1.1 Common master/slave image

If two interferograms share a common master/slave image, the decorrelation noise terms in the common image (e.g. the thermal and system noise terms in the shared image) appear in the interferometric phases of both interferograms, introducing correlation between them.

5.1.2 Common geometrical or Doppler-centroid decorrelation component

Even if there is nshared image between interferograms, the imaging geometry of the four acquisitions which produce the two interferograms, can cause correlation in the phase components of geometrical decorrelation, see e.g. Agram & Simons (2015). Assume the four SLC imagesP_1,P_2,P_3 and P_4 with the viewing geometry demonstrated in Figure 3. Then the total geometrical decorrelation noise affecting the interferometric phase ϕ_{34} also affects ϕ_{12} because of the overlap in the object spectrum, introducing correlation between the two interferometric phases. The same rationale can be also used for Doppler-centroid decorrelation, where an overlap in Doppler-baseline space can result in correlation between Doppler-centroid decorrelation phases in two interferograms.

5.1.3 Common temporal decorrelation component

An overlap between the time-period covered by two interferograms can cause correlation between components of temporal decorrelation. In other words, the changes in scattering characteristics of the surface during the common period of time affect the both interferograms in the same manner and may introduce a correlation between the temporal decorrelation phases.

5.2 Phase statistics for interferograms with a common image

In the case of only two interferometric phases constructed from three SLCs (i.e. ϕ_{12} and ϕ_{13} constructed from three SLCs in $y=[P_1,P_2,P_3]^T$ with absolute coherence matrix(Υ), Lucido et al. (2010) evaluated a closed form expression for the joint PDF of the two interferometric phases as

$$f_{\underline{\phi}_{12},\underline{\phi}_{13}}(\phi_{12},\phi_{13})=\frac{q}{(2\pi)^2|\Upsilon|^2\prod_{i=1}^{3}\lambda_{ii}}\ (1+q(I_{1,2,3}+I_{2,3,1}+I_{3,1,2})) \quad (22)$$

with the following variables: Elements of the inverse of the absolute coherence matrix λ_{ij} defined as

$$\Upsilon^{-1}=\begin{bmatrix}1 & |\gamma_{12}| & |\gamma_{13}|\\ |\gamma_{12}| & 1 & |\gamma_{23}|\\ |\gamma_{13}| & |\gamma_{23}| & 1\end{bmatrix}^{-1}=\begin{bmatrix}\lambda_{11} & \lambda_{12} & \lambda_{13}\\ \lambda_{12} & \lambda_{22} & \lambda_{23}\\ \lambda_{13} & \lambda_{23} & \lambda_{33}\end{bmatrix} \quad (23)$$

- parameter q defined as

$$q=\frac{1}{1-r_{12}^2-r_{13}^2-r_{23}^2+2r_{12}r_{13}r_{23}} \quad (24)$$

where

$$r_{ik}=r_{ki}=\frac{\lambda_{ik}\cos(\phi_{ik}-\phi_{0_{ik}})}{\sqrt{\lambda_{ii}\lambda_{kk}}} \quad (25)$$

- and $I_{i,k,l}$ given by

$$I_{i,k,l}=\frac{r_{ik}^3+2r_{il}r_{kl}-r_{ik}(1+r_{il}^2)+r_{kl}^2}{\sqrt{(1-r_{ik}^2)}}*\left(\frac{\pi}{2}-\arctan\left(\frac{r_{ik}}{\sqrt{(1-r_{ik}^2)}}\right)\right) \quad (26)$$

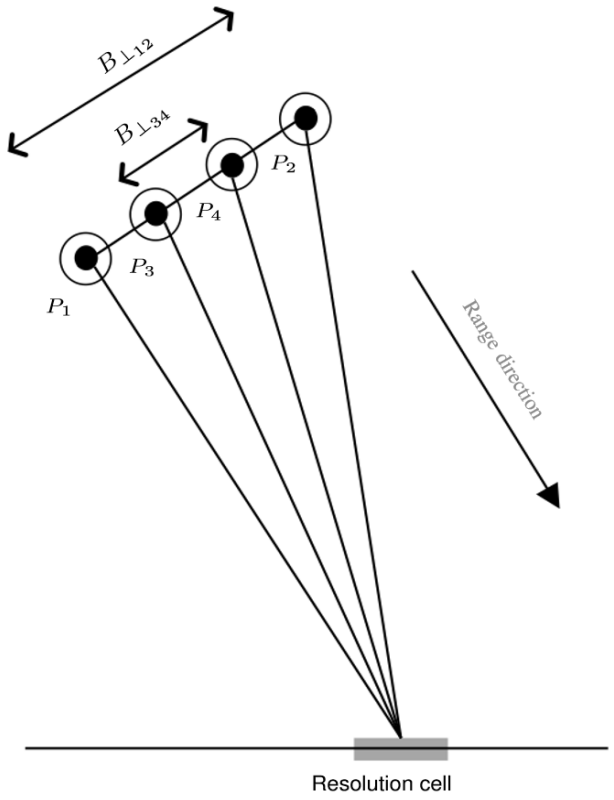

Figure 3. Example of InSAR acquisition geometry for four acquisitions P_1, P_2, $P_3$and P_4: demonstration of the cause of correlation between geometrical decorrelation phases in two interferograms. The total geometrical decorrelation noise affecting the interferometric phase ϕ_{34} also affects ϕ_{12} because of the overlap in the baseline space, introducing correlation between the two interferometric phases. Figure adapted from Agram & Simons (2015).

Note that the PDF of Eq. (22) is periodic with 2π cycles in two dimensions. Considering wrapped phases in the interval [-π, π), the peak/mode of the PDF is located at $[\phi_{0_{12}},\phi_{0_{13}}]^T$. Figure 4 shows examples of 2D representation of the joint PDF given by Eq. (22) for cases where the coherence between all SLC pairs assumed to be equal (i.e., $|\gamma_{12}|=|\gamma_{13}|=|\gamma_{23}|$), and for four different coherence values. Based on Eq. (22), the joint PDF of two interferometric phases sharing the same master image depends not only on the coherence values of the two interferograms, but also depends on the coherence of the third interferogram constructed by the two slave images. Figure 5 demonstrates this fact. In the plot, the coherence of two interferometric phases ϕ_{12} and ϕ_{13} is assumed to be constant and equal to $|\gamma_{12}|=|\gamma_{13}|=0.6$, but the coherence of the third interferogram (i.e. $|\gamma_{23}|$) is gradually increasing from 0.1 to 0.9. We can clearly see that the joint PDF of (and so the correlation between) the two interferometric phases varies depending on the value of the $|\gamma_{23}|$. Summarizing, in order to evaluate phase statistics of two interferometric phases constructed from three SLC values, the full 3×3 absolute coherence matrix ϒ is required. Note that Eq. (22) evaluates the joint PDF for two connected interferograms—sharing a common master/slave image—and only for single-look pixels. For more general cases, i.e., for two interferograms without a common image and for different multilooking factors, there is no closed-form expression available. For these cases, we will discuss the first two statistical moments of the joint-PDF in the next section.

5.3 First and second statistical moments

The expected value of the random vector of two interferometric phases (i.e., $\underline{y}= [\underline{\phi}_{12}, \underline{\phi}_{34}]^T$) is defined as a vector whose elements are the expected values of each interferometric phase, and so (see Eq. (19)).

$$\mathrm{E}\{\underline{y}\}=\mathrm{E}\left\{\begin{bmatrix}\underline{\phi}_{12}\\ \underline{\phi}_{34}\end{bmatrix}\right\}=\begin{bmatrix}\mathrm{E}\{\underline{\phi}_{12}\}\\ \mathrm{E}\{\underline{\phi}_{34}\}\end{bmatrix}=\begin{bmatrix}\phi_{0_{12}}\\ \phi_{0_{34}}\end{bmatrix} \tag{27}$$

The second statistical moment or dispersion of the vector $\underline{y}= [\underline{\phi}_{12}, \underline{\phi}_{34}]^T$ is defined as a 2×2 covariance matrix Q_y:

$$\mathrm{D}\{\underline{y}\}=\mathrm{D}\left\{\begin{bmatrix}\underline{\phi}_{12}\\ \underline{\phi}_{34}\end{bmatrix}\right\}=\mathrm{Q}_y=\begin{bmatrix}\sigma^2_{\underline{\phi}_{12}} & \sigma_{\underline{\phi}_{12},\underline{\phi}_{34}}\\ \sigma_{\underline{\phi}_{12},\underline{\phi}_{34}} & \sigma^2_{\underline{\phi}_{34}}\end{bmatrix}=$$

$$\int_{\mathrm{y}} (y-\mathrm{E}\{\underline{y}\})(y-\mathrm{E}\{\underline{y}\})^{\mathrm{T}} f_{\underline{y}}(y)\,dy \tag{28}$$

where $f_{\underline{y}}(y)$ represents the multivariate PDF of $\underline{y}$, i.e. $f_{\underline{y}}(y)=f_{\underline{\phi}_{12},\underline{\phi}_{34}}(\phi_{12},\phi_{34})$. The diagonal elements of this covariance matrix or the variance of the interferometric phases can be computed by numerical evaluation of Eq. (20) For multilooked pixels, or by evaluation of Eq. (21) For single-look cases. However, evaluation of the off-diagonal element or the covariance between interferometric phases requires numerical integration over the joint PDF:

$$\mathrm{Cov}\left\{\underline{\phi}_{12},\underline{\phi}_{34}\right\}=\sigma_{\underline{\phi}_{12},\underline{\phi}_{34}}=\int_{-\pi}^{\pi}\int_{-\pi}^{\pi}\phi_{12}\,\phi_{34}\mathrm{f}_{\underline{\phi}_{12},\underline{\phi}_{34}}(\phi_{12},\phi_{34})d\phi_{12}d\phi_{34} \tag{29}$$

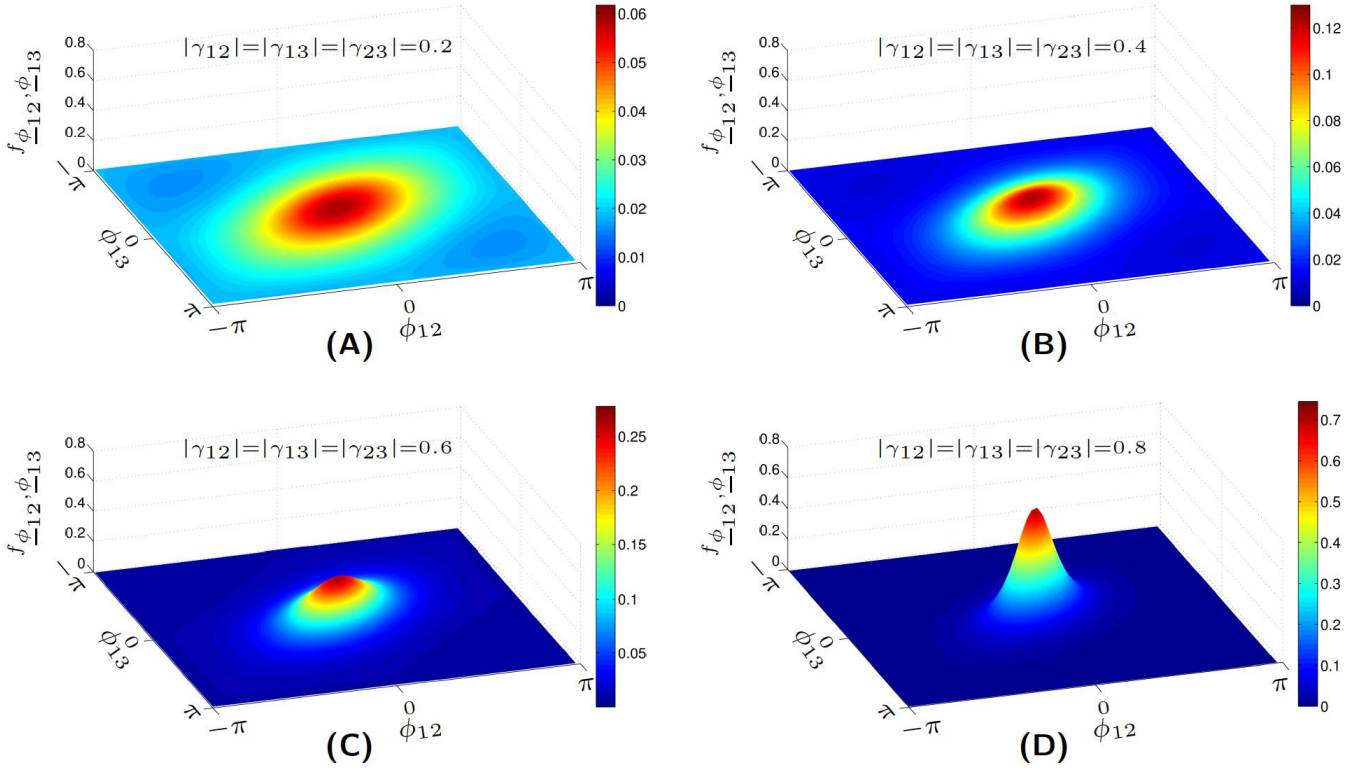

Figure 4. Examples of joint probability distribution function of two (single-look) interferometric phases ϕ_{12} and ϕ_{13} generated from three SLCs P_1,P_2, and P_3 with mutual coherence between all pairs of SLCs equal to (A) 0.2, (B) 0.4, (C) 0.6, and (D) 0.8, assuming $\phi_{0_{12}}$=0 and $\phi_{0_{13}}$=0. The PDFs are evaluated based on the closed form expression of Eq. (22). Colors denote the probability density. Note the difference in color scales.

Because the generic closed-form expression of the joint PDF is not available, Eqs. (29) or (28) cannot be evaluated. Therefore, the evaluation of the full phase covariance matrix requires an alternative approach. In the following, we present two approaches for this purpose: one based on the numerical Monte-Carlo integration and the other based on an analytical approximation using nonlinear error propagation.

5.4 Evaluation of phase covariance matrix: Monte-Carlo method

Monte-Carlo methods were originally developed for numerical evaluation of integrals by generating random numbers (Ripley .1987, Kalos and Whitlock .2008 and Liu .2001). More specifically for the computation of second statistical moment of interferometric phases, the integral of

$$\mathrm{D}\{\underline{y}\}=Q_y=\frac{1}{M}\sum_{i=1}^{M}(y^{(i)}-\mathrm{E}\{\underline{y}\})(y^{(i)}-\mathrm{E}\{\underline{y}\})^T \qquad (30)$$

where $y^{(i)}$,i=1…M are the M random realizations of vector $\underline{y}$ generated from multivariate PDF$f_{\underline{y}}(y)$.In order to generate random realizations of the vector of interferometric phases $y^{(i)}$, in the first step, random realizations of vector of SLC values (i.e., $\underline{y}_{\mathrm{slc}}$) are simulated from the multivariate circular Gaussian distribution specified by a coherence matrix. Subsequently, the sample vectors of interferometric phases are computed from the simulated SLC realizations. Finally the empirical covariance matrix is computed by Eq. (30) Based on the simulated realizations. The algorithm to compute the covariance matrix Q_y can be summarized as:

Inputs: the $N\times N$ absolute coherence matrix Υ (assuming a stack of N SLC images), the multilooking factor L, and the number of realizations M, which should be chosen as a large number. Eq. (28) can be numerically estimated by the Monte-Carlo integration as (Gundlich et al., 2003 ; Alkhatib, 2007).

Step 1: generate $M\times L$ vectors of samples $y_{\mathrm{slc}}^{(j)}$, j=1…$M\times L$ of the form of $y_{\mathrm{slc}}^{(j)}=[R_1^j\cdots R_N^{(j)}I_1^j\cdots I_N^{(j)}]^T$ from a zero-mean multivariate normal distribution[6] with absolute coherence matrix $Q_{y_{\mathrm{slc}}}=\frac{1}{2}\begin{bmatrix}\Upsilon & 0\\ 0 & \Upsilon\end{bmatrix}$

Step 2: compute M realizations of multilooked interferometric phase vectors $y^{(i)}$, i=1…M from $M\times L$ generated samples of SLC vectors $y_{\mathrm{slc}}^{(j)}$.

[6] Generating random samples from a multivariate normal distribution is a standard practice in numerical simulations, and there are various libraries and packages for it in different programming/statistical environments. An example is the function **mvnrnd.m** in the MATLAB statistical toolbox (MATLAB, 2014). For more information concerning methods and algorithms of generating random vectors from multivariate normal distribution, see, for example, the textbooks by (Gentle, 2003 ; Fishman, 2003).

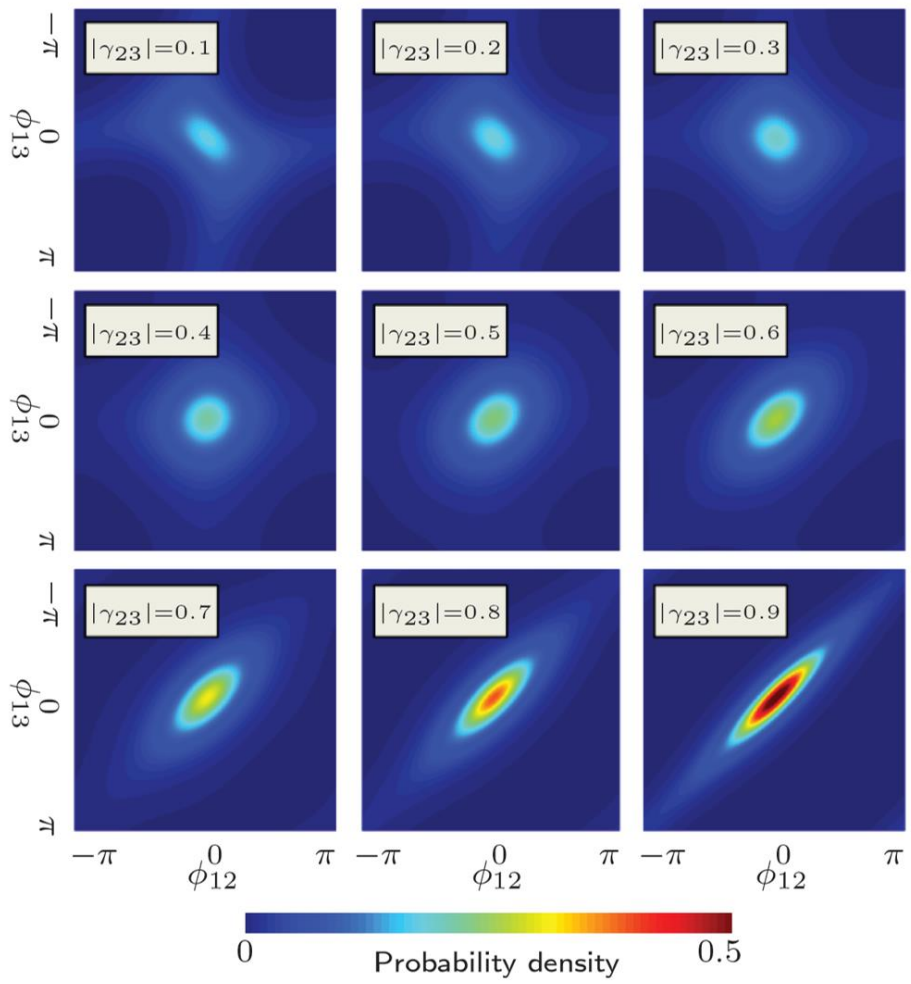

Step 3: compute the empirical covariance matrix by evaluation of Eq. (30), where the expectation $E\{\underline{y}\}$ can be estimated as the average of the simulated samples as $\hat{E}\{\underline{y}\}=1/M\sum_{i=1}^{M}\underline{y}^{(i)}$

Figure 5. Examples of joint probability distribution function of two (single-look) interferometric phases $\underline{\phi}_{12}$ and $\underline{\phi}_{13}$ generated from three SLCs P_1, P_2, and P_3. In all the plots, the coherence of $\underline{\phi}_{12}$ and $\underline{\phi}_{13}$ is assumed to be constant and equal to $|\gamma_{12}|=|\gamma_{13}|=0.6$, but the coherence of the connecting interferogram is gradually increasing from 0.1 to 0.9. This is the demonstration of the fact that the joint PDF of and the correlation between two interferometric phases (sharing a common master image) not only depends on the coherence of two interferograms but also depends on the coherence of the interferometric phase between the two slave images. (Colors denote the probability density).

Note that, although the integral of Eq. (28) was written for the vector of only two interferometric phases (i.e., $\underline{y}=[\underline{\phi}_{12},\underline{\phi}_{34}]^T$), the Monte-Carlo algorithm is generic and can be applied, in principle, to any stack of interferometric phases provided that an $N\times N$ absolute coherence matrix Υ is available.As a demonstration, for a stack of 10 SLC images, Figure 6 shows an arbitrary 10×10 coherence matrix Υ and its corresponding 45×45 covariance matrix Q_y computed by the Monte-Carlo method for the vector $\underline{y}$ which includes all the 45 interferometric combinations constructed from the 10 SLC images (assuming multilooking factor L=25). Note that the unit of interferometric phases is radian, so the unit of the elements of the covariance matrix is squared radians ([rad^2]).

5.5 Evaluation of phase covariance matrix: Analytical approximation

The closed-form evaluation of the second statistical moment of the vector of interferometric phases is challenging to derive due to the highly nonlinear relationship between SLC values and multilooked interferometric phases, and hence such a closed-form expression has not been derived so far. In this section, we derive such an expression using the concept of nonlinear error propagation in order to propagate the dispersion of SLC values described by coherence matrix to the dispersion of interferometric phases. Assume two complex interferograms $\underline{I}_{12}$ and $\underline{I}_{34}$ constructed from the set of four SLC values (i.e., $\underline{y}_{\text{slc}}=[\underline{P}_1,\underline{P}_2,\underline{P}_3,\underline{P}_4]^T$) with a circular complex Gaussian distribution described by a 4×4 absolute coherence matrix Υ

$$\Upsilon=\begin{bmatrix} 1 & |\gamma_{12}| & |\gamma_{13}| & |\gamma_{14}| \\ |\gamma_{12}| & 1 & |\gamma_{23}| & |\gamma_{24}| \\ |\gamma_{13}| & |\gamma_{23}| & 1 & |\gamma_{34}| \\ |\gamma_{14}| & |\gamma_{24}| & |\gamma_{34}| & 1 \end{bmatrix} \tag{31}$$

We are interested in the dispersion or covariance matrix of the vector of interferometric phases $\underline{y}=[\underline{\phi}_{12},\underline{\phi}_{34}]^T$. We assume, without loss of generality, that the amplitude of SLC images are normalized in the way that $E\{\underline{A}_i^2\}=1$ (Note that the final goal is the computation of the phase dispersion, which is invariant with respect to normalization of amplitudes). In the complex plain, every multilooked interferometric phase can be computed as the ratio between the multilooked interferometric imaginary component over the real component, and so:

$$\phi_{i,j}=\arctan\left(\frac{\Re(<I_{i,j}>)}{\Im(<I_{i,j}>)}\right) \tag{32}$$

where <.> denotes spatial complex averaging or complex multilooking. So the relationship between the vector of two interferometric phases (i.e., $\underline{y}=[\underline{\phi}_{12},\underline{\phi}_{34}]^T$) and interferometric real/imaginary components can be written as

$$\underline{y}=\begin{bmatrix}\underline{\phi}_{12}\\ \underline{\phi}_{34}\end{bmatrix}=\begin{bmatrix}\arctan\left(\frac{\Im(<\underline{I}_{1,2}>)}{\Re(<\underline{I}_{1,2}>)}\right)\\ \arctan\left(\frac{\Im(<\underline{I}_{3,4}>)}{\Re(<\underline{I}_{3,4}>)}\right)\end{bmatrix} \tag{33}$$

For simplicity, we express the vector of interferometric real and imaginary components as

$$\underline{x}=\begin{bmatrix}\underline{x}_1\\ \underline{x}_2\\ \underline{x}_3\\ \underline{x}_4\end{bmatrix}=\begin{bmatrix}\Re(<\underline{I}_{1,2}>)\\ \Re(<\underline{I}_{3,4}>)\\ \Im(<\underline{I}_{1,2}>)\\ \Im(<\underline{I}_{3,4}>)\end{bmatrix} \tag{34}$$

the functional relationship between the vector of two interferometric phases (i.e., $\underline{y}=[\underline{\phi}_{12},\underline{\phi}_{34}]^T$) and the vector

$$\underline{y}=\begin{bmatrix}\underline{\phi}_{12}\\ \underline{\phi}_{34}\end{bmatrix}=F(\underline{x})=\begin{bmatrix}F_1(\underline{x})\\ F_2(\underline{x})\end{bmatrix}=\begin{bmatrix}\arctan\left(\frac{\underline{x}_3}{\underline{x}_1}\right)\\ \arctan\left(\frac{\underline{x}_4}{\underline{x}_2}\right)\end{bmatrix} \tag{35}$$

Based on the nonlinear error propagation law, the dispersion of vector $\underline{y}=[\underline{\phi}_{12},\underline{\phi}_{34}]^T$ can be approximated as:

$$Q_y=\mathrm{D}\{\begin{bmatrix}\underline{\phi}_{12}\\ \underline{\phi}_{34}\end{bmatrix}\}\approx \mathrm{J_F}(x|x_0)\, Q_x\, J_F(x|x_0)^T \tag{36}$$

where $J_F(\underline{x}|x_0)$ is the Jacobian of the multivariate function $F(\underline{x})$ with respect to the vector $\underline{x}$ evaluated at an expected value x_0. For zero-mean[7] phases (i.e.,$\mathrm{E}\{\underline{\phi}_{1,2}\}=\mathrm{E}\{\underline{\phi}_{3,4}\}=0$), and assuming x_0 equal to the expected values of the interferometric real and imaginary components, Eq. (36) is evaluated and the dispersion or covariance matrix of the interferometric phase vector is approximated as (the explicit derivation is provided in Appendix A.

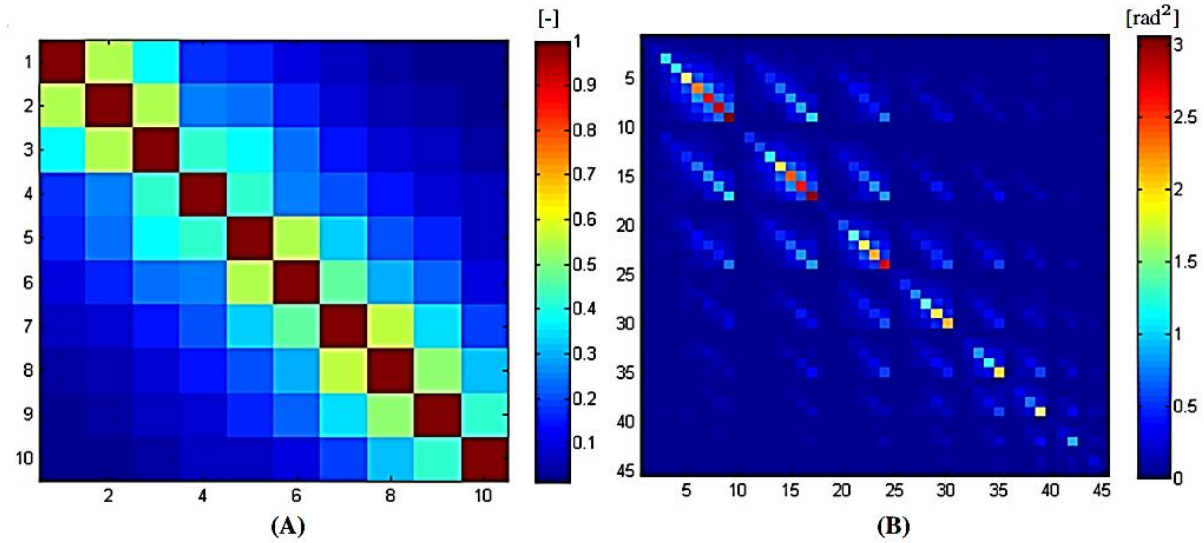

Figure 6. Demonstration of the Monte-Carlo method to propagate an absolute coherence matrix to interferometric phase covariance matrix: **(A)** An arbitrary 10×10 absolute coherence matrix$Y$, **(B)** corresponding 45×45 covariance matrix Q_y computed by the Monte-Carlo method for the vector of all the 45 interferometric combinations constructed from the 10 SLC images, for multilooking factor L=25. The 45 interferometric combinations in the vector y are assumed to be ordered as$\left[\phi_{12}\ldots\phi_{1N}\ \phi_{23}\ \ldots\phi_{2N}\ldots\phi_{(N-1)N}\right]$, where N=10.

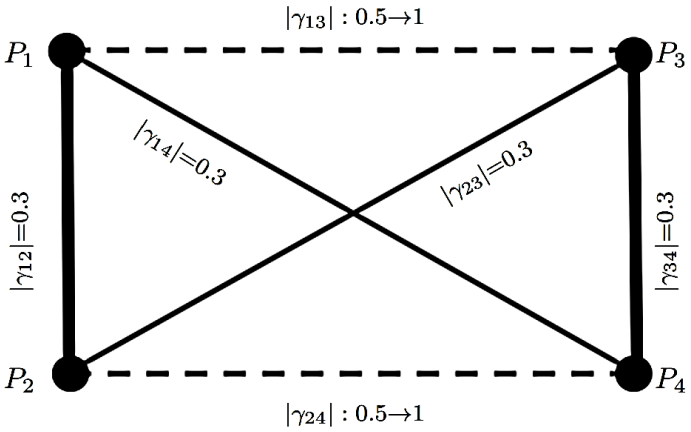

Figure 7. Stylized setting for the demonstration of covariance evaluation between two interferometric phases $\underline{\phi}_{12}$ and $\underline{\phi}_{34}$ (the results of simulation are visualized in Figure 8). Four SLC images P_1, P_2, P_3, and P_4 are considered, with absolute coherence values $|\gamma_{ij}|$. Four of the coherence values assumed to be constant and equal to an arbitrary value 0.3, and the coherence values $|\gamma_{13}|$ and $|\gamma_{24}|$ are gradually increased in the simulation from 0.5 to 1.

[7] Note that the assumption of zero mean phase is equivalent to changing the integration interval of Eqs. (15) and (16) to $(\phi_0-\pi,\phi_0+\pi)$ instead of $(-\pi,\pi)$ (see Section 4 and Eq. (20)).

$$\mathrm{D}\left\{\begin{bmatrix} \underline{L}_{12} \\ \underline{L}_{34} \end{bmatrix}\right\} \approx \begin{bmatrix} \frac{1-|\gamma_{12}|^2}{2L|\gamma_{12}|^2} & \frac{|\gamma_{13}||\gamma_{24}|-|\gamma_{14}||\gamma_{23}|}{2L|\gamma_{12}||\gamma_{34}|} \\ \frac{|\gamma_{13}||\gamma_{24}|-|\gamma_{14}||\gamma_{23}|}{2L|\gamma_{12}||\gamma_{34}|} & \frac{1-|\gamma_{34}|^2}{2L|\gamma_{34}|^2} \end{bmatrix} \quad (37)$$

from Eq. (37), the general equation for the interferometric phase variance and the covariance between interferometric phases are expressed as

$$\mathrm{D}\{\underline{\phi}_{ij}\} = \sigma^2_{\underline{\phi}_{ij}} \approx \frac{1-|\gamma_{ij}|^2}{2L|\gamma_{ij}|^2}, \quad (38)$$

and

$$\mathrm{Cov}\{\underline{\phi}_{ij},\underline{\phi}_{kl}\} = \sigma_{\underline{\phi}_{ij},\underline{\phi}_{kl}} \approx \frac{|\gamma_{ik}||\gamma_{jl}|-|\gamma_{il}||\gamma_{jk}|}{2L|\gamma_{ij}||\gamma_{kl}|}. \quad (39)$$

Note that, for two interferometric phases with the same master image, equation is reduced to

$$\mathrm{Cov}\{\underline{\phi}_{ij},\underline{\phi}_{ik}\} = \sigma_{\underline{\phi}_{ij},\underline{\phi}_{ik}} \approx \frac{|\gamma_{jk}|-|\gamma_{ij}||\gamma_{ik}|}{2L|\gamma_{ij}||\gamma_{ik}|}. \quad (40)$$

In a stack of N SLC images, for the vector of any subset of interferometric phases, all the elements of the full covariance matrix of interferometric phases can be approximated by Eqs. (38), (39), and provided that the $N\times N$ absolute coherence matrix is available. In summary, with these two equations, the absolute coherence matrix Υ can be approximately propagated to the full covariance matrix of the multilooked interferometric phases. It should be pointed out that the approximation via nonlinear error propagation is valid when the dispersion of interferometric real/imaginary components is relatively small with respect to nonlinearity of the function $F(\underline{x})$ around its expectation. This assumption holds for high coherence values or a large number of looks. This is in fact the reason that the variance of Eq. (38) gives exactly the variance of interferometric phase of point scatterers, which have a relatively large interferometric amplitude compared to dispersion of their interferometric real/imaginary components. As a demonstration for covariance evaluation between two interferometric phases $\underline{\phi}_{12}$ and $\underline{\phi}_{34}$, we simulate some numerical examples. The setting of the simulation has been captured in Figure 7 Four SLC images P_1,P_2, P_3, and P_4 are considered, with absolute coherence values $|\gamma_{ij}|$. Four of the coherence values are assumed to be constant and equal to an arbitrary value of 0.3, and the coherence values $|\gamma_{13}|$ and $|\gamma_{24}|$ are gradually increased in the simulation from 0 to 1. The results of the simulation for four different multilooking factors L=1,5,20 and 50 are visualized in Figure 8. We can clearly see that Eq. (39) provides an good approximation for high number of looks. This is expected as, for larger L, the dispersion of interferometric real and imaginary components gets smaller and so the nonlinear error propagation gives a better approximation. Rocca (2007) and De Zan et al. (2015) also have reported as equation for the evaluation of covariance between interferometric phases as:

$$\mathrm{Cov}\{\underline{\phi}_{ij},\underline{\phi}_{kl}\} \approx \frac{|\gamma_{il}||\gamma_{jk}|-|\gamma_{ij}||\gamma_{kl}|}{2L|\gamma_{ij}||\gamma_{kl}|}. \quad (41)$$

Note the difference between the numerators of Eqs. (41) and (39). It is possible to show that Eq. (41) derived by (Rocca, 2007; De Zan et al., 2015) has been derived based on the simplified assumption that complex interferograms have a circular complex distribution, which is an invalid assumption as the Hermitian product of circularly Gaussian distributed SLC values does not generally follow a circular distribution (see Appendix A). Furthermore, we can see that Eq. (39) is truly the function of all the six absolute coherence values in Υ, in contrast with Eq. (41) which is invariant with respect to the coherence values $|\gamma_{ik}|$ and $|\gamma_{jl}|$. For example, for the demonstration setting of Figure 7, Eq. (41) evaluates the covariance values equal to zero which is clearly wrong compared to the results of the Monte-Carlo simulation (see Figure 8). Hence, we conclude that Eq. (39) is more generic than Eq. (41) and is a better approximation for the phase covariance of interferometric phases.

6. Summary and conclusions

This paper gave an overview of single-point statistics for distributed scatterers in InSAR stacks. We reviewed the single-point statistics of interferometric phase values, for both cases of a single interferogram (Section 4) and a stack of interferograms (Section 5). For a vector of (multilooked) interferometric phases associated with a single DS-pixel, the stochastic model has been given in terms of second statistical moments or the covariance matrix. We have introduced a Monte-Carlo numerical approach to evaluate the covariance matrix of interferometric phases (Section 5.4). As an alternative, an analytical approximation for evaluation of the variances and covariance's of interferometric phases has been also derived by nonlinear propagation of SAR statistics (i.e., coherence matrix) into the dispersion of interferometric phases (Section 5.5).

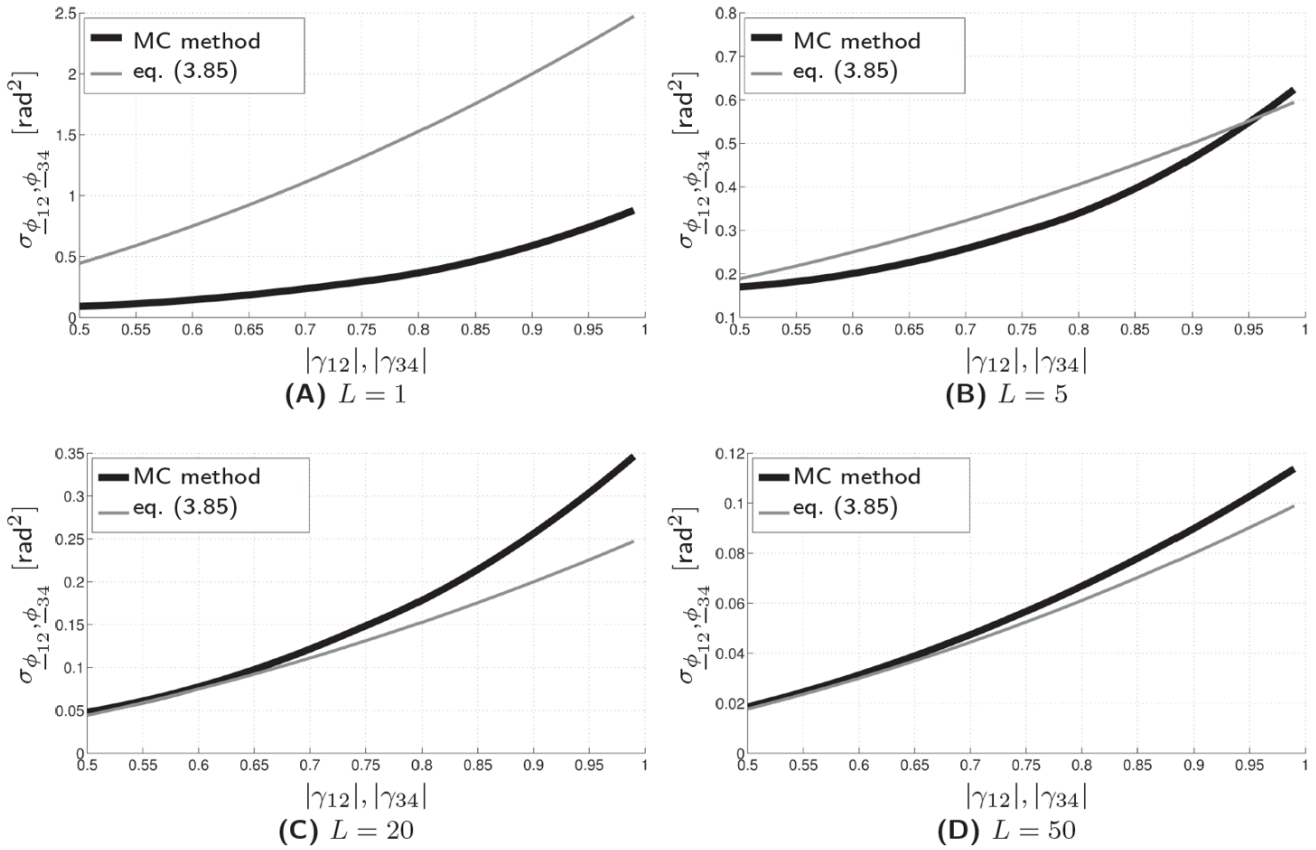

Figure 8. Demonstration of covariance evaluation between two interferometric phases $\underline{\phi}_{12}$ and $\underline{\phi}_{34}$, and comparison between evaluations by the Monte-Carlo approach and the closed-form evaluation of Eq. (39), for four different multilooking factors: **(A)** L = 1, **(B)** L = 5, **(C)** L = 20, and **(D)** L = 50. The stylized setting of the demonstration have been visualized in Figure 7. We can see for higher number of looks, Eq. (39) provides a good approximation

Appendix A: Derivation of Equation (37)

The objective is to evaluate the covariance matrix of the vector $\underline{y}=[\underline{\phi}_{12},\underline{\phi}_{34}]^T$ via the approximation (nonlinear error propagation):

$$\underline{Q}_y=\mathrm{D}\{\begin{bmatrix}\underline{\phi}_{12}\\ \underline{\phi}_{34}\end{bmatrix}\}\approx J_F(x|x_0)\,\underline{Q}_x\,J_F(x|x_0)^T \tag{42}$$

- where x is the vector of interferometric real and imaginary components as

$$\underline{x}=\begin{bmatrix}\underline{x}_1\\ \underline{x}_2\\ \underline{x}_3\\ \underline{x}_4\end{bmatrix}=\begin{bmatrix}\Re(<\underline{I}_{1,2}>)\\ \Re(<\underline{I}_{3,4}>)\\ \Im(<\underline{I}_{1,2}>)\\ \Im(<\underline{I}_{3,4}>)\end{bmatrix} \tag{43}$$

- $F(\underline{x})$ is the multivariate function describing the relationship between the vector of two interferometric phases (i.e., $\underline{y}=[\underline{\phi}_{12},\underline{\phi}_{34}]^T$) and $\underline{x}$:

$$\underline{y}=\begin{bmatrix}\underline{\phi}_{12}\\ \underline{\phi}_{34}\end{bmatrix}=F(\underline{x})=\begin{bmatrix}F_1(\underline{x})\\ F_2(\underline{x})\end{bmatrix}=\begin{bmatrix}\arctan(\frac{\underline{x}_3}{\underline{x}_1})\\ \arctan(\frac{\underline{x}_4}{\underline{x}_2})\end{bmatrix} \tag{44}$$

- And $J_F(\underline{x}|x_0)$ is the Jacobian of the multivariate function $F(\underline{x})$ with respect to the vector $\underline{x}$ evaluated at an initial value x_0.

Derivation of $J_F(\underline{x}|x_0)$:

The Jacobian of $J_F(\underline{x})$ is computed by taking the partial derivatives of F with respect to the elements of $\underline{x}$, so

$$J_F(\underline{x})=\begin{bmatrix}\frac{\underline{x}_3}{\underline{x}_1^2+\underline{x}_3^2} & 0 & \frac{\underline{x}_1}{\underline{x}_1^2+\underline{x}_3^2} & 0\\ 0 & \frac{\underline{x}_4}{\underline{x}_2^2+\underline{x}_4^2} & 0 & \frac{\underline{x}_2}{\underline{x}_2^2+\underline{x}_4^2}\end{bmatrix} \tag{45}$$

The initial value x_0 can be selected at the expected value of the elements of $\underline{x}$:

$$x_0=\begin{bmatrix}x_{0_1}\\ x_{0_2}\\ x_{0_3}\\ x_{0_4}\end{bmatrix}=\begin{bmatrix}\mathrm{E}\{\Re(<\underline{I}_{1,2}>)\}\\ \mathrm{E}\{\Re(<\underline{I}_{3,4}>)\}\\ \mathrm{E}\{\Im(<\underline{I}_{1,2}>)\}\\ \mathrm{E}\{\Im(<\underline{I}_{3,4}>)\}\end{bmatrix} \tag{46}$$

Assuming zero-mean interferometric phase (i.e. $\mathrm{E}\{\underline{\phi}_{12}\}=\mathrm{E}\{\underline{\phi}_{34}\}=0$), the elements of x_0 are evaluated as:

$$x_0=\begin{bmatrix}x_{0_1}\\ x_{0_2}\\ x_{0_3}\\ x_{0_4}\end{bmatrix}=\begin{bmatrix}|\gamma_{12}|\\ |\gamma_{34}|\\ 0\\ 0\end{bmatrix} \tag{47}$$

Evaluating the Jacobian of Eq. (45) at x_0 gives

$$J_F(\underline{x}|x_0)=\begin{bmatrix}0 & 0 & \frac{1}{|\gamma_{12}|} & 0\\ 0 & 0 & 0 & \frac{1}{|\gamma_{34}|}\end{bmatrix} \quad (48)$$

Derivation of Q_x:

First, it should be noted that, generally speaking, complex interferograms that are computed by the Hermitian product of circularly Gaussian distributed SLC values, do not follow a circular distribution, and hence, the multivariate PDF of the vector of complex interferometric values may not be circular. In general, for a non-circularly distributed random vector z, the dispersion or covariance matrix defined as $\mathrm{D}\{\underline{z}\}=\mathrm{E}\{\underline{z}\underline{z}^*\}$ does not entirely describe the second order statistics of $\underline{z}$ (Mandic & Goh, 2009). This is due to the fact that the vector z and its conjugate transpose z^* are correlated in case of non-circularity. For a full description of the second statistical moment of non-circularly distributed complex vectors, a complementary quantity called *pseudo-covariance* or *complementary covariance* needs to be taken into account (Mandic & Goh, 2009 ; Neeser & Massey, 1993; Picinbono & Bondon, 1997; Schreier & Scharf, 2003). The complementary covariance is defined as $\mathrm{E}\{\underline{z}\underline{z}^T\}$ where the $.^T$ denotes the standard transpose operation. In agreement with the terminology *complementary covariance*, we introduce the term *complementary dispersion* denoted by $\tilde{\mathrm{D}}$ which is defined as $\tilde{\mathrm{D}}\{\underline{z}\}=\mathrm{E}\{\underline{z}\underline{z}^T\}$. It is known that the dispersion of the vector of real and imaginary component of $\underline{z}$ can be computed as (Neeser & Massey, 1993).

$$\mathrm{D}\left\{\begin{bmatrix}\Re(\underline{z})\\ \Im(\underline{z})\end{bmatrix}\right\}=\begin{bmatrix}\frac{1}{2}\Re(\mathrm{D}\{\underline{z}\}+\tilde{\mathrm{D}}\{\underline{z}\}) & \frac{1}{2}\Im(\mathrm{D}\{\underline{z}\}+\tilde{\mathrm{D}}\{\underline{z}\})\\ -\frac{1}{2}\Im(\mathrm{D}\{\underline{z}\}-\tilde{\mathrm{D}}\{\underline{z}\}) & \frac{1}{2}\Re(\mathrm{D}\{\underline{z}\}-\tilde{\mathrm{D}}\{\underline{z}\})\end{bmatrix} \quad (49)$$

Assuming the complex vector of the interferometric phases $\underline{z}=[\underline{I}_{12},\underline{I}_{34}]^T$, the vector $\underline{x}$ can be reformulated as

$$\underline{x}=\begin{bmatrix}\Re(\underline{z})\\ \Im(\underline{z})\end{bmatrix} \quad (50)$$

And so the dispersion of $\underline{x}$ (i.e., Q_x) can be evaluated by Eq. (49). In order to evaluate Eq. (49), the dispersion and the complementary dispersion of $\underline{z}=[\underline{I}_{12},\underline{I}_{34}]^T$ should be derived. The dispersion of $\underline{z}=[\underline{I}_{12},\underline{I}_{34}]^T$ is written as

$$\mathrm{D}\{\underline{z}\}=\mathrm{D}\left\{\begin{bmatrix}\underline{I}_{12}\\ \underline{I}_{34}\end{bmatrix}\right\} \quad (51)$$

$$=\mathrm{D}\left\{\begin{bmatrix}\underline{P}_1\underline{P}_2^*\\ \underline{P}_3\underline{P}_4^*\end{bmatrix}\right\} \quad (52)$$

$$=\mathrm{E}\left\{\begin{bmatrix}\underline{P}_1\underline{P}_2^*\\ \underline{P}_3\underline{P}_4^*\end{bmatrix}\begin{bmatrix}\underline{P}_2\underline{P}_1^* & \underline{P}_4\underline{P}_3^*\end{bmatrix}\right\} \quad (53)$$

$$=\begin{bmatrix}\mathrm{E}\{\underline{P}_1\underline{P}_2^*\underline{P}_2\underline{P}_1^*\} & \mathrm{E}\{\underline{P}_1\underline{P}_2^*\underline{P}_4\underline{P}_3^*\}\\ \mathrm{E}\{\underline{P}_2\underline{P}_1^*\underline{P}_3\underline{P}_4^*\} & \mathrm{E}\{\underline{P}_3\underline{P}_4^*\underline{P}_4\underline{P}_3^*\}\end{bmatrix} \quad (54)$$

Using the Gaussian moment factoring theorem[8] Reed (1962) and Krishnan & Chandra (2006), Eq. (54) is written as:

$$\mathrm{D}\{\underline{z}\}=\begin{bmatrix}\mathrm{E}\{\underline{P}_1\underline{P}_2^*\}\mathrm{E}\{\underline{P}_2\underline{P}_1^*\}+\mathrm{E}\{\underline{P}_1\underline{P}_1^*\}\mathrm{E}\{\underline{P}_2^*\underline{P}_2\} & \cdots\\ \mathrm{E}\{\underline{P}_2\underline{P}_1^*\}\mathrm{E}\{\underline{P}_3\underline{P}_4^*\}+\mathrm{E}\{\underline{P}_2\underline{P}_4^*\}\mathrm{E}\{\underline{P}_1^*\underline{P}_3\} & \\ \mathrm{E}\{\underline{P}_1\underline{P}_2^*\}\mathrm{E}\{\underline{P}_4\underline{P}_3^*\}+\mathrm{E}\{\underline{P}_1\underline{P}_3^*\}\mathrm{E}\{\underline{P}_2^*\underline{P}_4\} & \\ \mathrm{E}\{\underline{P}_3\underline{P}_4^*\}\mathrm{E}\{\underline{P}_4\underline{P}_3^*\}+\mathrm{E}\{\underline{P}_3\underline{P}_3^*\}\mathrm{E}\{\underline{P}_4^*\underline{P}_4\} & \end{bmatrix} \quad (55)$$

Assuming amplitude-normalized SLC images (i.e $\mathrm{E}\{\underline{A}_I^2\}=1$ and zero-mean interferometric phases (i.e. $\mathrm{E}\{\phi_{i,j}\}=0$), the expected value of the interferograms is equal to the absolute coherence values (i.e., $\mathrm{E}\{\underline{P}_i\underline{P}_j^*\}=\mathrm{E}\{\underline{P}_j\underline{P}_i^*\}=|\gamma_{i,j}|$,see Eq. (5) and so Eq. (55) can be evaluated as:

$$\mathrm{D}\{\underline{z}\}=\mathrm{D}\left\{\begin{bmatrix}\underline{I}_{12}\\ \underline{I}_{34}\end{bmatrix}\right\}=\begin{bmatrix}1+|\gamma_{12}|^2 & |\gamma_{12}||\gamma_{34}|+|\gamma_{13}||\gamma_{24}|\\ |\gamma_{12}||\gamma_{34}|+|\gamma_{13}||\gamma_{24}| & 1+|\gamma_{34}|^2\end{bmatrix} \quad (56)$$

In the same manner the complementary dispersion of $\underline{z}$ is computed as Eq. (57):

$$\tilde{\mathrm{D}}\{\underline{z}\}=\tilde{\mathrm{D}}\left\{\begin{bmatrix}\underline{I}_{12}\\ \underline{I}_{34}\end{bmatrix}\right\}=\tilde{\mathrm{D}}\left\{\begin{bmatrix}\underline{P}_1\underline{P}_2^*\\ \underline{P}_3\underline{P}_4^*\end{bmatrix}\right\}=\mathrm{E}\left\{\begin{bmatrix}\underline{P}_1\underline{P}_2^*\\ \underline{P}_3\underline{P}_4^*\end{bmatrix}\begin{bmatrix}\underline{P}_2\underline{P}_1^* & \underline{P}_4\underline{P}_3^*\end{bmatrix}\right\}=\begin{bmatrix}\mathrm{E}\{\underline{P}_1\underline{P}_2^*\underline{P}_2\underline{P}_1^*\} & \mathrm{E}\{\underline{P}_1\underline{P}_2^*\underline{P}_4\underline{P}_3^*\}\\ \mathrm{E}\{\underline{P}_2\underline{P}_1^*\underline{P}_3\underline{P}_4^*\} & \mathrm{E}\{\underline{P}_3\underline{P}_4^*\underline{P}_4\underline{P}_3^*\}\end{bmatrix}=$$
$$\begin{bmatrix}\mathrm{E}\{\underline{P}_1\underline{P}_2^*\}\mathrm{E}\{\underline{P}_2\underline{P}_1^*\}+\mathrm{E}\{\underline{P}_1\underline{P}_1^*\}\mathrm{E}\{\underline{P}_2^*\underline{P}_2\} & \mathrm{E}\{\underline{P}_1\underline{P}_2^*\}\mathrm{E}\{\underline{P}_4\underline{P}_3^*\}+\mathrm{E}\{\underline{P}_1\underline{P}_3^*\}\mathrm{E}\{\underline{P}_2^*\underline{P}_4\}\\ \mathrm{E}\{\underline{P}_2\underline{P}_1^*\}\mathrm{E}\{\underline{P}_3\underline{P}_4^*\}+\mathrm{E}\{\underline{P}_2\underline{P}_4^*\}\mathrm{E}\{\underline{P}_1^*\underline{P}_3\} & \mathrm{E}\{\underline{P}_3\underline{P}_4^*\}\mathrm{E}\{\underline{P}_4\underline{P}_3^*\}+\mathrm{E}\{\underline{P}_3\underline{P}_3^*\}\mathrm{E}\{\underline{P}_4^*\underline{P}_4\}\end{bmatrix}$$
$$=\begin{bmatrix}2|\gamma_{12}|^2 & |\gamma_{12}||\gamma_{34}|+|\gamma_{14}||\gamma_{23}|\\ |\gamma_{12}||\gamma_{34}|+|\gamma_{14}||\gamma_{23}| & 2|\gamma_{34}|^2\end{bmatrix} \quad (57)$$

Substituting Eqs. (56) and (57) into Eq. (49) gives the dispersion of x (for single-look pixels). Finally for

[8] Gaussian moment factoring theorem: if $\underline{x}_1$, $\underline{x}_2$, $\underline{x}_3$, and $\underline{x}_4$ are zero mean variables with a complex jointly Gaussian distribution, the following relationship holds:
$\mathrm{E}\{\underline{x}_1\underline{x}_2^*\underline{x}_3\underline{x}_4^*\}=\mathrm{E}\{\underline{x}_1\underline{x}_2^*\}\mathrm{E}\{\underline{x}_3\underline{x}_4^*\}+\mathrm{E}\{\underline{x}_1\underline{x}_4^*\}\mathrm{E}\{\underline{x}_2^*\underline{x}_3\}$

multilooked pixels computed by coherent averaging over L independent homogeneous pixels with covariance

$$D\{\underline{x}\}=\phi_x=\frac{1}{2}\begin{bmatrix} 3|\gamma_{12}|^2+1 & 2|\gamma_{12}||\gamma_{34}|+\dots \\ & |\gamma_{13}||\gamma_{34}|+|\gamma_{14}||\gamma_{23}| \\ 2|\gamma_{12}||\gamma_{34}|+\dots & 3|\gamma_{12}|^2+1 \\ |\gamma_{13}||\gamma_{34}|+|\gamma_{14}||\gamma_{23}| & \\ 0 & 0 \\ 0 & 0 \end{bmatrix} \begin{matrix} 0 & 0 \\ 0 & 0 \\ 1-|\gamma_{12}|^2 & |\gamma_{13}||\gamma_{24}|-|\gamma_{14}||\gamma_{23}| \\ |\gamma_{13}||\gamma_{24}|-|\gamma_{14}||\gamma_{23}| & 1-|\gamma_{12}|^2 \end{matrix} \tag{58}$$

matrix Q_X: the covariance matrix of the vector of interferometric real and imaginary components is computed by linear error propagation as

$$Q_{x|L}=\frac{1}{L}Q_x \tag{59}$$

Derivation of Q_y:

By substituting Eqs. (59), (58), and (48) into Eq. (42), the covariance matrix of the interferometric phase vector is approximated as

$$\mathrm{D}\left\{\begin{bmatrix}\underline{\phi}_{12}\\ \underline{\phi}_{34}\end{bmatrix}\right\}\approx\begin{bmatrix} \frac{1-|\gamma_{12}|^2}{2L|\gamma_{12}|^2} & \frac{|\gamma_{13}||\gamma_{24}|-|\gamma_{14}||\gamma_{23}|}{2L|\gamma_{12}||\gamma_{34}|} \\ \frac{|\gamma_{13}||\gamma_{24}|-|\gamma_{14}||\gamma_{23}|}{2L|\gamma_{12}||\gamma_{34}|} & \frac{1-|\gamma_{34}|^2}{2L|\gamma_{34}|^2} \end{bmatrix} \tag{60}$$

References

Ferretti, A., Fumagalli, A., Novali, F., Prati, C., Rocca, F., & Rucci, A. (2011). A new algorithm for processing interferometric data-stacks: SqueeSAR. IEEE Transactions on Geoscience and Remote Sensing, 49(9), 3460-3470.

Guarnieri, A. M., & Tebaldini, S. (2008). On the exploitation of target statistics for SAR interferometry applications. IEEE Transactions on Geoscience and Remote Sensing, 46(11), 3436-3443.

Bamler, R., & Hartl, P. (1998). Synthetic aperture radar interferometry. Inverse problems, 14(4), R1.

Tough, R. J. A., Blacknell, D., & Quegan, S. (1995, June). A statistical description of polarimetric and interferometric synthetic aperture radar data. In Proceedings of the Royal Society of London A: Mathematical, Physical and Engineering Sciences (Vol. 449, No. 1937, pp. 567-589). The Royal Society.

Just, D., & Bamler, R. (1994). Phase statistics of interferograms with applications to synthetic aperture radar. Applied optics, 33(20), 4361-4368.

Lee, J. S., Hoppel, K. W., Mango, S. A., & Miller, A. R. (1994). Intensity and phase statistics of multilook polarimetric and interferometric SAR imagery. IEEE Transactions on Geoscience and Remote Sensing, 32(5), 1017-1028.

Rodriguez, E., & Martin, J. M. (1992, April). Theory and design of interferometric synthetic aperture radars. In IEE Proceedings F (Radar and Signal Processing) (Vol. 139, No. 2, pp. 147-159). IET Digital Library.

Sarabandi, K. (1992). Derivation of phase statistics from the Mueller matrix. *Radio Science*, *27*(05), 553-560.

Eineder, M., & Adam, N. (2005). A maximum-likelihood estimator to simultaneously unwrap, geocode, and fuse SAR interferograms from different viewing geometries into one digital elevation model. IEEE Transactions on Geoscience and Remote Sensing, 43(1), 24-36.

Cuenca, M. C., Hooper, A. J., & Hanssen, R. F. (2011). A new method for temporal phase unwrapping of persistent scatterers InSAR time series. IEEE Transactions on Geoscience and Remote Sensing, 49(11), 4606-4615.

Lucido, M., Meglio, F., Pascazio, V., & Schirinzi, G. (2010). Closed-form evaluation of the second-order statistical distribution of the interferometric phases in dual-baseline SAR systems. IEEE Transactions on Signal Processing, 58(3), 1698-1707.

Hanssen, R. F. (2001). Radar interferometry: data interpretation and error analysis (Vol. 2). Springer Science & Business Media.

Ferretti, A., Prati, C., & Rocca, F. (2001). Permanent scatterers in SAR interferometry. IEEE Transactions on geoscience and remote sensing, 39(1), 8-20.

Kampes, B. M., & Hanssen, R. F. (2004). Ambiguity resolution for permanent scatterer interferometry. IEEE Transactions on Geoscience and Remote Sensing, 42(11), 2446-2453.

Danvenport Jr, W. B. (1970). Probability and random processes and introduction for applied scientists and engineers (No. 519.2 D3).

Madsen, S. N. (1986). Speckle theory: Modelling, analysis, and applications related to synthetic aperture radar data. Ph. D thesis, Electromagnetics Institute, 62.

Goodman, J. W. (1976). Some fundamental properties of speckle. JOSA, 66(11), 1145-1150.

Hannan, E. J., & Thomson, P. J. (1971). The estimation of coherence and group delay. Biometrika, 58(3), 469-481.

Born, M., & Wolf, E. (2013). Principles of optics: electromagnetic theory of propagation, interference and diffraction of light. Elsevier.

Foster, M. R., & Guinzy, N. J. (1967). The coefficient of coherence: its estimation and use in geophysical data processing. Geophysics, 32(4), 602-616.

Papoulis, A. (1985). Random Variables and Stochastic Processes.

Goodman, N. R. (1963). Statistical analysis based on a certain multivariate complex Gaussian distribution (an introduction). The Annals of mathematical statistics, 34(1), 152-177.

Barber, B. C. (1993). The phase statistics of a multichannel radar interferometer. Waves in random media, 3(4), 257-266.

Gradshteyn, I. S., & Ryzhik, I. M. (2014). Table of integrals, series, and products. Academic press.

Joughin, L. R., & Winebrenner, D. P. (1994, August). Effective number of looks for a multilook interferometric phase distribution. In Geoscience and Remote Sensing Symposium, 1994. IGARSS'94. Surface and Atmospheric Remote Sensing: Technologies, Data Analysis and Interpretation., International(Vol. 4, pp. 2276-2278). IEEE.

Oberhettinger, F. (1972). Hypergeometric functions. Handbook of mathematical functions, 556.

Abramowitz, M., & Stegun, I. A. (1966). Handbook of mathematical functions. Applied mathematics series, 55(62), 39.

Quegan, S., Dutra, L. V., & Grover, K. (1994). Phase measurements in MAESTRO polarimetric data from the UK test sites. International Journal of Remote Sensing, 15(14), 2719-2736.

Agram, P. S., & Simons, M. (2015). A noise model for InSAR time series. Journal of Geophysical Research: Solid Earth, 120(4), 2752-2771.

Ripley, B. D. (2009). Stochastic simulation (Vol. 316). John Wiley & Sons.

Kalos, M. H., & Whitlock, P. A. (2008). Monte carlo methods. John Wiley & Sons.

Liu, J. S. (2008). Monte Carlo strategies in scientific computing. Springer Science & Business Media.

Gundlich, B., Koch, K. R., & Kusche, J. (2003). Gibbs sampler for computing and propagating large covariance matrices. Journal of Geodesy, 77(9), 514-528.

Alkhatib, H. (2008). On Monte Carlo methods with applications to the current satellite gravity missions (Doctoral dissertation, Universität Bonn).

MATLAB, version R2014a, statistical toolbox. Natick, Massachusetts: The MathWorks Inc., 2014.

Gentle, J. E. (2006). Random number generation and Monte Carlo methods. Springer Science & Business Media.

Fishman, G. (2013). Monte Carlo: concepts, algorithms, and applications. Springer Science & Business Media.

Rocca, F. (2007). Modeling interferogram stacks. IEEE Transactions on Geoscience and Remote Sensing, 45(10), 3289-3299.

De Zan, F., Zonno, M., & López-Dekker, P. (2015). Phase inconsistencies and multiple scattering in SAR interferometry. IEEE Transactions on Geoscience and Remote Sensing, 53(12), 6608-6616.

Mandic, D. P., & Goh, V. S. L. (2009). Complex valued nonlinear adaptive filters: noncircularity, widely linear and neural models (Vol. 59). John Wiley & Sons.

Neeser, F. D., & Massey, J. L. (1993). Proper complex random processes with applications to information theory. IEEE transactions on information theory, 39(4), 1293-1302.

Picinbono, B., & Bondon, P. (1997). Second-order statistics of complex signals. IEEE Transactions on Signal Processing, 45(2), 411-420.

Schreier, P. J., & Scharf, L. L. (2003). Second-order analysis of improper complex random vectors and processes. IEEE Transactions on Signal Processing, 51(3), 714-725

Reed, I. (1962). On a moment theorem for complex Gaussian processes. IRE Transactions on Information Theory, 8(3), 194-195.

Krishnan, V. (2015). Probability and random processes. John Wiley & Sons.